THE STUDY OF THE INTERACTION MECHANISM OF LINOLEIC ACID AND 1-LINOLEYL-2-OLEOYL-3-LINOLENOYL-GLYCEROL WITH FE$_3$O$_4$ NANOPARTICLES

Iryna Tsykhanovska[1] , Victoria Evlash[2], Alexandr Alexandrov[1], Tatyana Gontar[1], Daniil Shmatkov[1]*

Abstract. The interaction mechanism of Fe$_3$O$_4$ nanoparticles with linoleic acid and 1-linoleyl-2-oleoyl-3-linolenoyl-glycerol represented by two-layer coordination model has been determined. By means of Fourier spectroscopy, scanning electron microscopy, energy dispersive X-ray spectroscopy, X-ray photoelectron spectroscopy, X-ray phase and thermal gravitational analysis, the interaction mechanism of lipids (linoleic acid and sunflower oil) with Fe$_3$O$_4$ nanoparticles has been studied.

Keywords: Fe$_3$O$_4$ nanoparticles, linoleic acid, 1-linoleyl-2-oleoyl-3-linolenoyl-glycerol, sunflower oil, chemisorption.

1. Introduction

One of the important operational and technological properties of the food raw materials and food ingredients that determines the technological processes course and the finished product quality is the fat holding capacity (FHC). FHC is the capacity to bind and hold fats which are triglycerides. Apart from triglycerides, the edible fats contain the higher fatty acids (oleinic, linoleic and linolneic acids in oils; palmitic and stearic acids in animal fats). Therefore, when studying the FHC mechanism, it is necessary to consider the physicochemical interactions of the food system ingredients with the main components of fats and oils – triglycerides and the higher fatty acids. Knowledge of the binding mechanisms will allow to rationally use the new types of food raw materials and additives, as well as to predict the behavior of ingredients in the food systems (dough and confectionery masses, minced meat, *etc*.) during processing and storage of the finished products.

The food fibers have the high fat binding capacity (FBC), the mechanism of which is not well studied. There is an opinion that FHC and FBC are determined by lignin presence and independent from its particles size [1, 2]. Some authors [3-6] showed the dependence of fat holding and binding capacities on the number and size of the raw material particles. This suggested that the mechanism of fat absorption by the food fibers can be determined not only by the lignin sorption activity, the efficiency of which increases when grinding, but also by the surface adsorption [3-6].

The numerous studies show that the structure peculiarities and the presence of hydrophobic groups contribute to the fat binding by the raw material components [3-8]. By the experimental studies the good FHC was found for citrus fibers Herbacel AQ Plus, type N and Citrifi; carrageenans; carob bean, guar and xanthan gums [7-9]; the egg powder, the milk powder and the dairy foods; wheat, soya, oatmeal and pea flour [7, 9, 10]; various functional ingredients derived from the industrial by-products (skin, hoof, feathers, by-products, *etc*.) [9, 11]; and the oil based functional gels [12, 13]. First grade flour binds and holds the fats better compared with top quality flour due to the higher content of proteins and food fibers in it. Carrageenans contain hydrophilic and hydrophobic groups providing their ability to bind and hold fats. FHC of milk powder and dairy foods is provided by the presence of casein, which has both the hydrophobic and hydrophilic sites [7]. Recently, various nanopowder food additives, in particular, silver, iron oxides, titanium dioxide, and silicon dioxide, have been used to improve FHC of the food systems [14-21]. This ability is associated with the high dispersion, which allows not only to bind free fats, but also to hold them on the nanoparticles surface while cooking, as well as with a good accessibility of numerous hydrophobic sites [14-17].

In the scientific works [18-20] a model of monolayer adsorption (chemisorption) of fatty acids on the nanoparticles surface of the metal oxides is proposed. A model of two-layer adsorption is also considered: the

[1] Ukrainian Engineering Pedagogic Academy,
16, Universitetskaya St., 61003 Kharkiv, Ukraine
[2] Kharkiv State University of Food Technology and Trade,
333, Klochkovskaya St., 61051, Kharkiv, Ukraine
* *cikhanovskaja@gmail.com*

first monolayer occurs on the nanoparticle surface due to the chemisorption of fatty acids and makes the particles superhydrophobic; the second layer occurs due to the interaction of hydrophobic sites of the first monolayer with the alkyl substituents of fatty acids [21]. However, these assumptions are controversial and require the additional experimental confirmation.

The analysis of literary sources [1-21] showed that there are insufficient data on the FHC mechanism by the nanopowder food additives, in particular, Fe_3O_4 nanoparticles. Fe_3O_4 nanopowder is a major component of Magnetofood food additive developed by the authors of this work.

The nanopowder based on Fe_3O_4 (Magnetofood) has the great potential and new operational and technological properties (emulsifying, water-binding, water-holding, fat-binding, fat-holding) and promising technological applications [16, 17, 22-25]. The interaction of Magnetofood nanoparticles with the biopolymers of the food systems (proteins, proteids, carbohydrates, lipids) is a system of complex chemical reactions. The supramolecular organization of Fe_3O_4 nanoparticles and the organic matrix structure play the important role. The result is the formation of spatial nanostructures which significantly affect the functional and technological properties of the raw materials and semi-finished products (confectionery and dough masses, minced meat, *etc.*) [16, 17, 23, 25].

Therefore, the works on the creation of the new operational and technological properties of the food systems with the help of the nanopowder food additives of the complex action are topical. At the same time, it is important to understand the mechanisms of main properties formation, including FHC. To explain the FHC mechanism by Fe_3O_4 nanoparticles of Magnetofood, it is necessary to understand the nature of Fe_3O_4 nanoparticles interaction with triglycerides and the higher fatty acids.

So, the purpose of this work is the study of the interaction mechanism of linoleic acid and triglyceride – 1-linoleyl-2-oleoyl-3-linolenoyl-glycerol with Fe_3O_4 nanoparticles.

2. Experimental

2.1. Materials

Five samples were used for the investigations.

Sample 1. High-dispersive black colored powder of Fe_3O_4 with the particles size of ~78 nm. The sample was obtained according to the technology developed by us [15] *via* the reaction of chemical co-precipitation of the iron salts in an alkaline medium.

Sample 2. Linoleic acid purchased from Reakhim, Ukraine.

Sample 3. Crude sunflower oil purchased from Vinnytska industrial company ViOil, Ukraine or 1-linoleyl-2-oleoyl-3-linolenoyl-glycerol obtained *via* the esterification reaction of glycerol with non-saturated fatty acids (linoleic, oleic and linolenic) laboratory of the Department of Chemical and Food Technologies of Ukrainian Engineering Pedagogics Academy.

Sample 4. Fe_3O_4 nanoparticles coated with linoleic acid. They were obtained by the dispersion of 1 g of Fe_3O_4 nanoparticles (sample 1) and 0.2 g of linoleic acid in 10 ml of dimethylformamide for 12 h at (323 ± 1) K under nitrogen stream blowing over the reaction mixture surface. After cooling the suspension to 293–298 K, Fe_3O_4 nanoparticles coated with linoleic acid were separated by magnetic filtration and washed with the water-ethanol mixture (1: 1) 5–7 times. The final product was dried in a vacuum at 333 ± 1 K for 24 h.

Sample 5. Fe_3O_4 nanoparticles coated with crude sunflower oil or 1-linoleyl-2-oleoyl-3-linolenoyl-glycerol. They were obtained by the procedure analogous to the previous one with the only difference that crude sunflower oil or 1-linoleyl-2-oleoyl-3-linolenoyl-glycerol was taken instead of linoleic acid.

2.2. Research Methods

2.2.1. IR-Fourier spectroscopy (FTIR)

A Tensor 37 Fourier spectrometer (Bruker, Germany), controlled by the OPUS software package with the standard graduated capabilities in the frequency range of 4000–400 cm^{-1} in the absorption format was used. Spectra of samples 1, 4, 5 were recorded in the KBr tablets; samples 2, 3 – in the "liquid film").

2.2.2. X-ray diffraction analysis (XRD)

XRD of the experimental samples 1, 4, 5 was performed using a powder diffractometer Siemens D500 (Germany) in the copper radiation with a graphite monochromator. The researches were carried out according to the well-known Bragg-Brenton technique [26]. The sample was dried at room temperature (293 K), thoroughly ground and mixed in a mortar. Then the sample was transferred to $2 \times 1 \times 0.1$ mm^3 glass cuvette to record the diffractogram. The angle range was $10° < 2\theta < 150°$ with the step of 0.02° and an accumulation time of 12 s at each point. The primary phase search was performed by using the PDF-4 card file [27], and then the roentgenogram was calculated using the Ritveld method.

2.2.3. Transmission electron microscopy (**TEM**)

For samples 1, 4 and 5 the particles size and morphology were determined by using a JSM-820

scanning electron microscope (JEOL, Japan) with the magnification of 150000. The obtained images in a planar geometry with the electron beam falling along the hexagonal axis and perpendicular to it were processed with the help of AutoCAD 2014 and MathCad 2014 programs. Based on the obtained results, the particle distribution was calculated relative to the diameter. To determine the average values the particles number in the sample was at least 500.

2.2.4. Energy dispersive X-ray spectroscopy (EDX)

To determine the elemental composition of the experimental samples 1, 4 and 5, a scanning electron microscope JSM-820 (JEOL, Japan) with an EDX connector was used. X-ray spectra were obtained by bombarding experimental samples with electrons using an acceleration voltage of 20 kV (corresponding to the lines of the characteristic spectra of Fe, C and O).

2.2.5. X-ray photoelectron spectroscopy (XPS)

The chemical composition of the surface layers and the chemical state of the elements on the surface of samples 4 and 5 were determined using a Kratos Axis Ultra DLD electron spectrometer (Kratos Analytical Ltd, UK). The exciting X-ray was the Al K_α line with photon energy $hv = 1486.6$ eV, tube voltage was 15 kV, the emission current was 10 mA. General XPS-spectra were recorded under constant energy mode of 160 eV and spectra of the internal electronic levels of the main elements Fe 2p, O 1s, C 1s – of 40 eV. The scale of the binding energy (E_b) was pre-calibrated according to the position of the main levels peaks Au $4f_{5/2}$ ($E_b = 83.96$ eV), Ag $3d_{5/2}$ ($E_b = 368.21$ eV) and Cu $2p_{3/2}$ ($E_b = 932.62$ eV); calibration accuracy was ±0.03 eV. Samples charge was evaluated according to carbon C 1s spectra (284.5 eV).

The samples were prepared by embedding thin layer of the sample (~50.0 mg) into metallic indium, which is located directly in the holder of the measuring unit of the device.

For a detailed analysis of the atoms chemical states we used spectra decomposition by the individual components according to the program that takes into account the mixed Lorentz-Gaussian shape of the peaks and the area under the peaks with simultaneous optimization of the background parameters. At the same time the minimizing principle of the bands number needed to describe the experimental spectra was used.

The error in the peak position determining was ±0.01 eV. To analyze the atoms chemical state (Fe, O, C) on the samples surface the spectra of the electronic levels Fe 2p (705–740 eV), O 1s (525–554 eV) and C 1s (275–295 eV) were studied in detail and thus the phase composition of the samples surface was quantified.

2.2.6. Thermogravimetric analysis (TGA)

The thermogravimetric investigations of samples 4 and 5 (~5.0 mg) were carried out using a Q-1500D derivatograph (IOM, Hungary) within the temperature range of 293–1173 K) at a heating rate of 5 K/min. An aluminum oxide ($T = 1473$ K) was used as a standard.

3. Results and Discussion

3.1. Substantiation of the Interaction Mechanism of Linoleic Acid and 1-Linoleyl-2-Oleoyl-3-Linolenoyl-Glycerol with Fe₃O₄ Nanoparticles

Adsorption (chemisorption) of the higher fatty acids and triglycerides on the Fe_3O_4 nanoparticles surface is mainly determined by electrostatic – dipole-dipole (Van der Waals forces), ion-dipole and ionic interactions. The donor-acceptor (coordination) interactions are also involved in the adsorption of fats and oils. The interactions appear between the Fe_3O_4 nanoparticles surface and triglyceride and the adsorbed free fatty acids. It means that under the influence of Fe_3O_4 nanoparticles the fats and oils undergo the structural changes affecting the fat holding and binding processes.

The RHC mechanism of Fe_3O_4 nanoparticles can be presented by the two-layer coordination model. The first adsorption layer is formed on the nanoparticle surface due to the electrostatic interactions of polarized lipid groups with ionized Fe_3O_4 particles and the coordination bonds of Fe atoms of Fe_3O_4 nanoparticles with the carbonyl and hydroxyl O atoms of the carboxyl groups of the free fatty acids, as well as with O atoms of ester groups of triglycerides. The second adsorption layer occurs due to the electrostatic hydrophobic interactions of the hydrophobic centers of the first monolayer and the aliphatic side chains of the acyl residues of triglycerides and the alkyl components of the free fatty acids.

The Fe^{2+} and Fe^{3+} cations of Fe_3O_4 magnetic nanoparticles are the structure-forming ions. The high intensity of the electric field generated by iron ions of Fe_3O_4 enhances the polarization of the triglyceride molecules and free fatty acids, which contributes to the additional ordering of bond dipoles $C^{\delta+}= O^{\delta-}$ and $O^{\delta-}- H^{\delta+}$ outside the surface of Fe_3O_4 particles and lipid adsorption.

Fig. 1 shows the types of the ionized Fe_3O_4 nanoparticles (NP). There are opposite polarized areas (Fe "+" and O "–", Fig. 1a) on the surface of Fe_3O_4 NP. In the presence of H^+ protons, originating in the acidic media during the hydrolysis of edible fats and oils, the formation of the protonated Fe_3O_4 NP is possible (Fig. 1b). These

particles appear as a coordination bond (oxygen of Fe_3O_4 is a donor, H^+ proton of the medium is an acceptor). The energy of the coordination bond is 50–200 kJ/mol. The protonated Fe_3O_4 particles can form the bonds of ion-ion (energy ~100–400 kJ/mol) and ion-dipole (energy ~50–200 kJ/mol) types with ions and the polarized molecules of free lipids (fatty acids and triglycerides) [16, 17, 20].

The ionized Fe_3O_4 particles are capable of chemical and electrostatic interactions (Figs. 2, 3). In Fig. 2 the ionic interactions between the ionized Fe_3O_4 nanoparticles and the charged carboxyl group (COO^-) of the higher fatty acids are represented. They are characterized by the high binding energy (~500–1000 kJ/mol) [16, 17, 20].

Probable ion-dipole interactions of Fe_3O_4 nanoparticles with the ionic groups of triglycerides and free fatty acids are shown in Fig. 3. These interactions occur between the protonated NP ($Fe_3O_4H^+$) and oxygen of hydroxyl and carbonyl groups of free fatty acids carboxylate; alcohol and carbonyl oxygen of triglyceride ester group.

Fig. 4 shows the dipole-dipole interactions of Fe_3O_4 nanoparticles with the ionic groups of triglycerides and free fatty acids. The energy of the dipole-dipole (Van der Waals) interaction is small – about 5–50 kJ/mol [16, 17, 20]. The dipole-dipole interactions are possible between the polarized Fe_3O_4 nanoparticle ("$^+$"Fe_3O_4"$^-$") and dipole of hydroxyl ($^{-\delta}O - H^{\delta+}$) and carbonyl ($^{-\delta}O = C^{\delta+}$) group of free fatty acids carboxylate; alcoholic ($^{-\delta}O - C^{\delta+}$) and carbonyl ($^{-\delta}O = C^{\delta+}$) dipoles of triglycerides ester group.

The interaction of Fe_3O_4 nanoparticles with the polarized carboxyl groups of free fatty acids and ester groups of triglyceride is also possible due to the coordination bonds.

Under the influence of Fe_3O_4 nanoparticles the fats and oils undergo the structural changes and form together stable complexes. Fig. 5 shows the process of nanoparticles self-organization in electrostatic complexes with linoleic acid and with 1-linoleyl-2-oleoyl-3-linolenoyl-glycerol, which are stabilized by the coordination (donor-acceptor) bonds of Fe and O atoms.
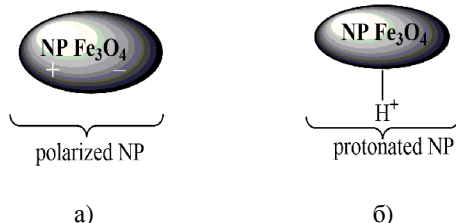
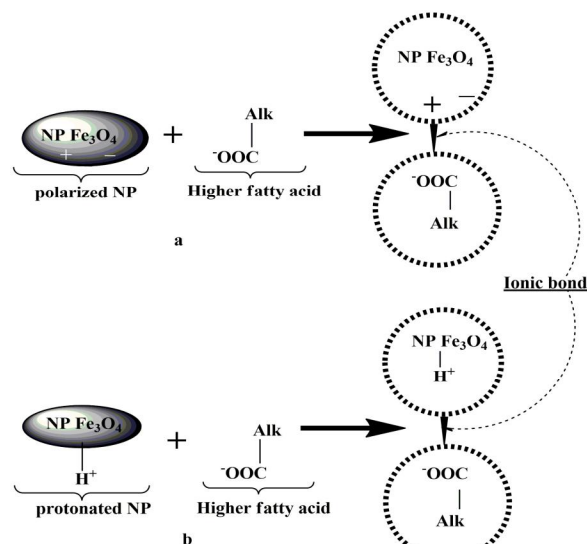**Fig. 1.** Polarized (a) and protonated (b) Fe_3O_4 nanoparticles

Fig. 2. The ionic interactions between the polarized (a) and protonated (b) Fe_3O_4 nanoparticles and COO^- group of the higher fatty acids
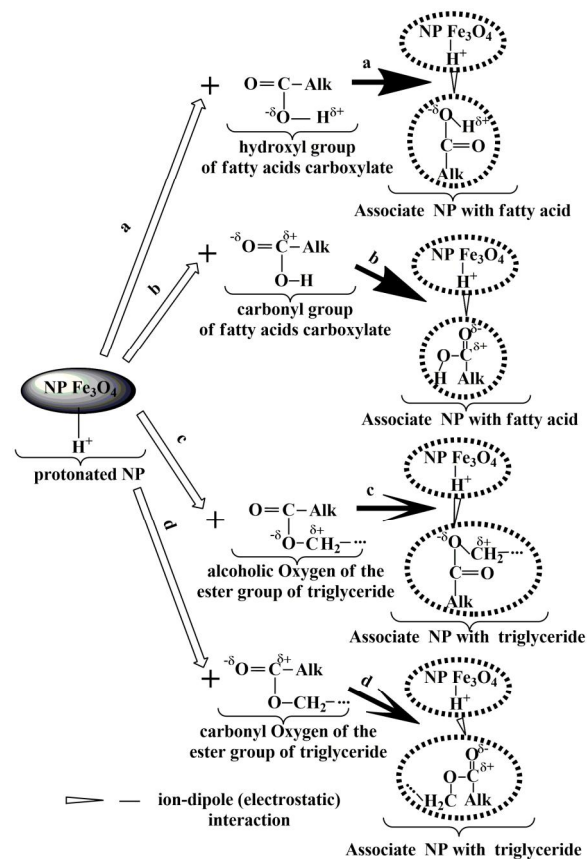
Fig. 3. The ion-dipole interaction between protonated Fe_3O_4 nanoparticle ($Fe_3O_4H^+$) and oxygen of carboxylate hydroxyl group of free fatty acids (a); oxygen of carboxylate carbonyl group of free fatty acids (b); alcoholic oxygen of triglyceride ester group (c) and carbonyl oxygen of triglyceride ester group (d)
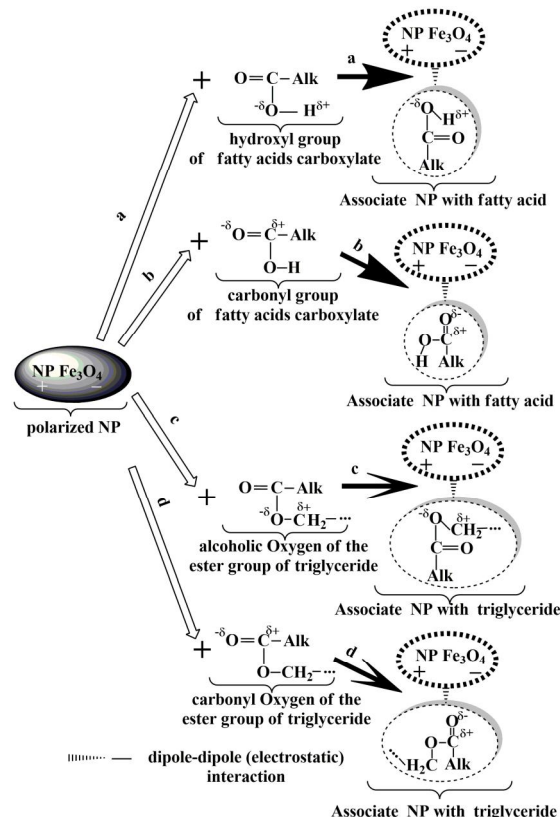
Fig. 4. The dipole-dipole interaction between the polarized Fe$_3$O$_4$ nanoparticles ($^{+}$Fe$_3$O$_4$$^{-}$) and dipole of the hydroxyl group ($^{-\delta}O - H^{\delta+}$) of free fatty acids carboxylate (a); dipole of the carbonyl group ($^{-\delta}O = C^{\delta+}$) of free fatty acids carboxylate (b); alcohol dipole ($^{-\delta}O - C^{\delta+}$) of triglyceride ester group (c) and carbonyl dipole ($^{-\delta}O = C^{\delta+}$) of triglyceride ester group (d)

From data of Fig. 5 it should be noted that Fe$_3$O$_4$ nanoparticles form the electrostatic complexes due to the coordination bonds with the oxygen atoms of carboxylate (the interaction with linoleic acid) and ester (the interaction with triglyceride – 1-linoleyl-2-oleoyl-3-linolenoyl-glycerol) groups.

The ability of Fe$_3$O$_4$ nanoparticles to enter into the electrostatic (Figs. 2-4) and coordination (Fig. 5) interaction with the hydrophilic centers of free fatty acids and triglycerides causes the chemisorption of the ionized Fe$_3$O$_4$ NP on the reactive surface. As a result, the first adsorption layer is formed on the particles surface. Taking into account all mentioned above and previous studies regarding the chemical reactions of the metal oxides nanoparticles and carboxylates of the higher fatty acids, the model of interaction between the hydrophilic centers of triglycerides and fatty acids with Fe$_3$O$_4$ NP can be represented by four types: ionic (Fig. 2), monodentate (Fig. 6), bidentate (chelate) (Fig. 7), and bidentate (bridge) (Fig. 8) [16, 17, 20].

It is obvious from Fig. 6 that due to the complex interaction (electrostatic and coordination) one Fe cation of Fe$_3$O$_4$ binds to one carboxylic oxygen atom of fatty (linoleic) acid (Fig. 6a) or to one esteric oxygen atom of triglyceride (1-linoleyl-2-oleoyl-3-linolenoylg-lycerol) (Fig. 6b). As a result, the monodirectional electrostatic complex is formed.

The bidentate electrostatic complex (Fig. 7) in which one Fe cation of Fe$_3$O$_4$ is bound with two oxygen atoms of the linoleic acid carboxyl group or the ester group of 1-linoleyl-2-oleoyl-3-linolenoyl-glycerol is formed due to the complex interaction (electrostatic and coordination).
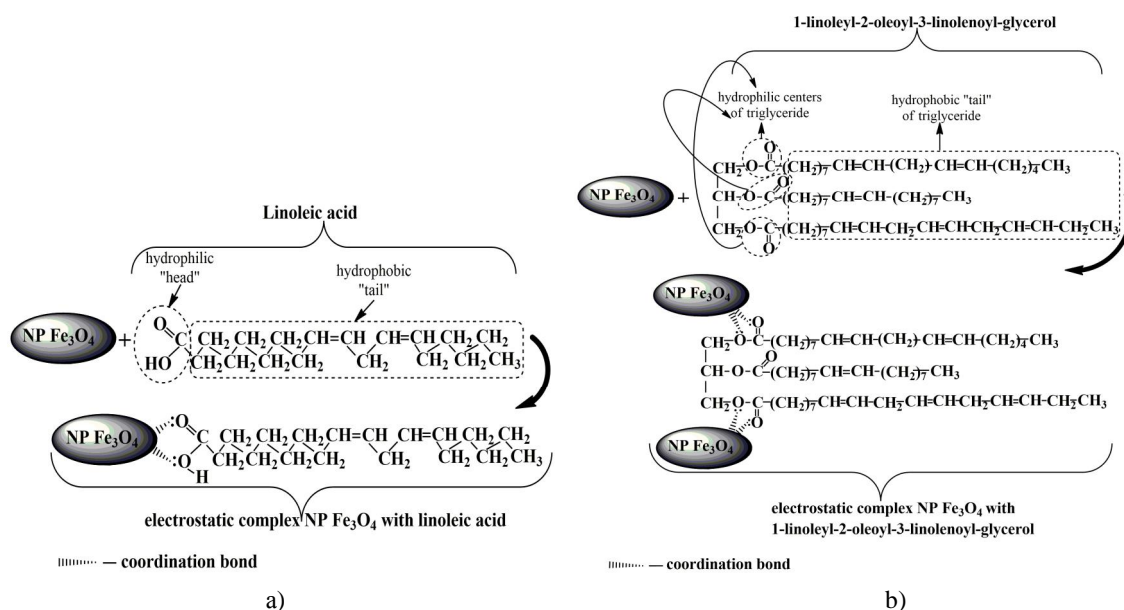

Fig. 5. The formation of electrostatic complex Fe$_3$O$_4$ nanoparticles with linoleic acid (a) and 1-linoleyl-2-oleoyl-3-linolenoyl-glycerol (b)
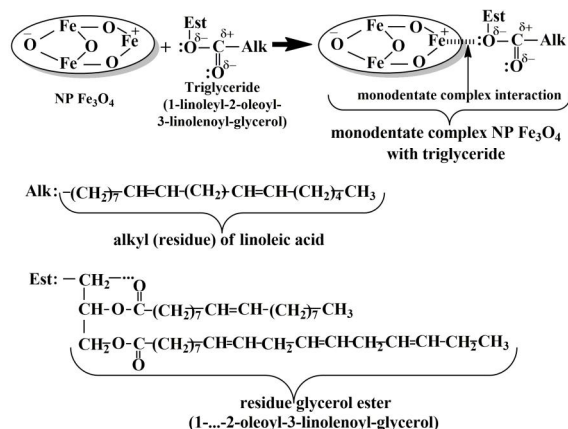
Iryna Tsykhanovska et al.

Fig. 6. The formation of monodentate complex Fe$_3$O$_4$ nanoparticles with fatty (linoleic) acid (a)
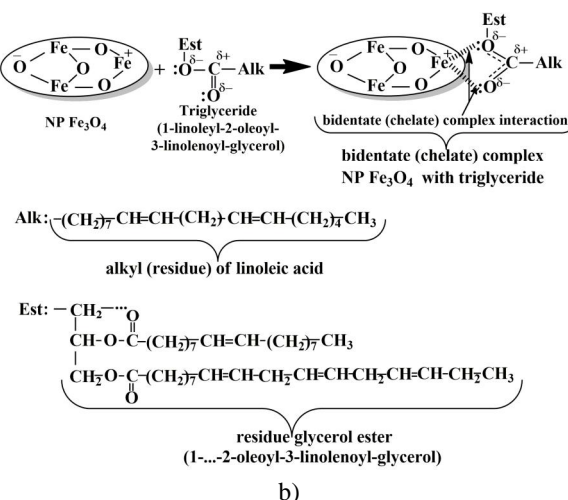and triglyceride (1-linoleyl-2-oleoyl-3-linolenoylglycerol) (b)

Fig. 7. The formation of bidentate (chelate) complex Fe$_3$O$_4$ nanoparticles with fatty (linoleic) acid (a)
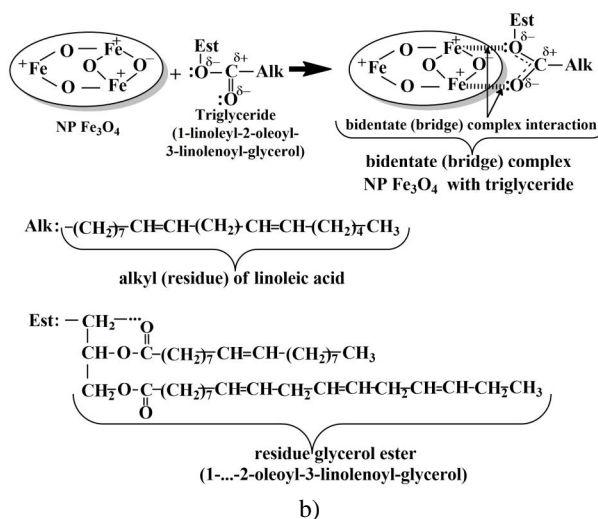and triglyceride (1-linoleyl-2-oleoyl-3-linolenoylglycerol) (b)

Fig. 8. The formation of bidentate (bridge) complex Fe$_3$O$_4$ nanoparticles with fatty (linoleic) acid (a)
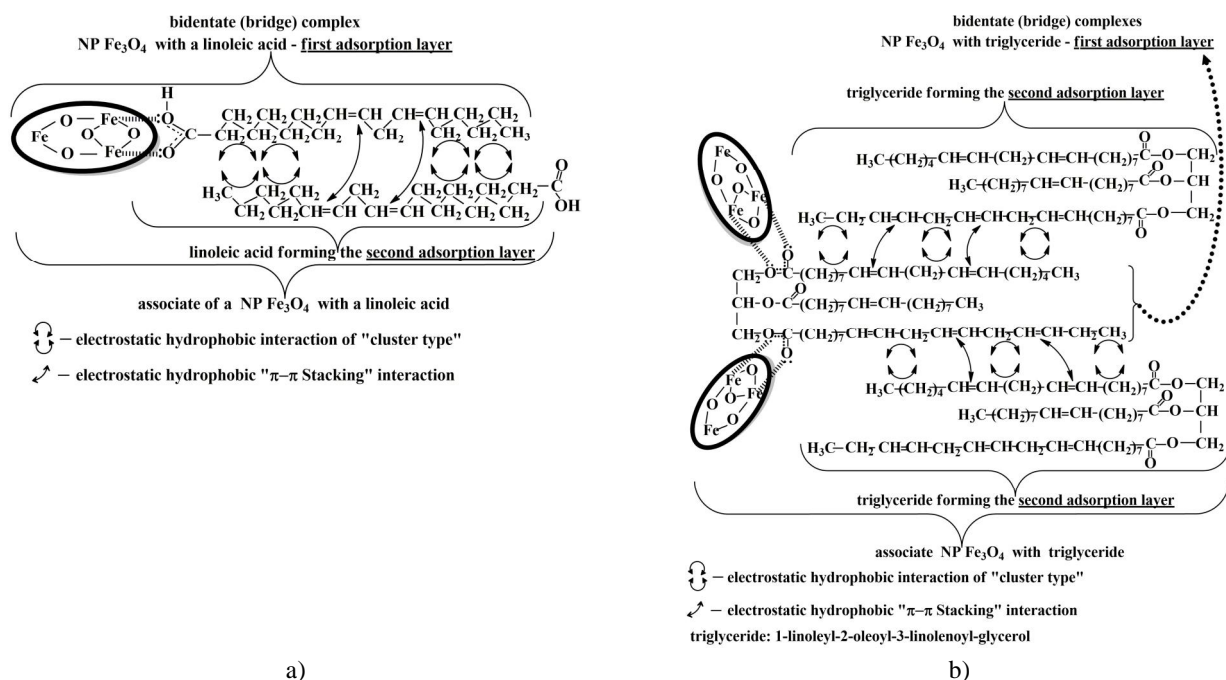and triglyceride (1-linoleyl-2-oleoyl-3-linolenoylglycerol) (b)

Fig. 9. The formation of Fe$_3$O$_4$ nanoparticles lipid associate with linoleic acid (a) and 1-linoleyl-2-oleoyl-3-linolenoylglycerol (b)

The formation mechanism of the bidentate (bridge) complex Fe$_3$O$_4$ nanoparticles with linoleic acid and 1-linoleyl-2-oleoyl-3-linolenoylglycerol is shown in Fig. 8. In this model two Fe cations of Fe$_3$O$_4$ are bound with two oxygen atoms (carboxyl group of linoleic acid or ester group of 1-linoleyl-2-oleoyl-3-linolenoylglycerol) due to the complex interaction.

The first adsorption layer, which is formed as a result of electrostatic and coordination interactions (Figs. 2-8), is hydrophobic due to alkyl hydrophobic residues ("tails") of the fatty acids (in particular, linoleic acid) and triglycerides (in particular, 1-linoleyl-2-oleoyl-3-linolenoyl-glycerol).

Then, the second adsorption layer is formed owing to the electrostatic hydrophobic interaction. The hydrophobic matrix of the first adsorption layer enters into the electrostatic hydrophobic interaction with hydrophobic aliphatic "tails" of fatty acids and triglycerides.

The Fe$_3$O$_4$ NP-lipid associate is formed due to the hydrophobic interactions. The formation mechanism is represented in Fig. 9. Long molecules of the higher fatty acids and triglycerides give the possibility for multicentered dispersion interaction. As a result, the lipid alkyl matrix is structured according to Van der Waals complexes. The matrix forms the second adsorption layer and the associate of Fe$_3$O$_4$ NP with lipids.

3.2. Experimental Studies of the Lipid interaction with Fe$_3$O$_4$ Nanoparticles

3.2.1. IR- Fourier Spectroscopy (FTIR)

To establish the adsorption interaction mechanism of the lipid molecules (in particular, linoleic acid and sunflower oil) with Fe$_3$O$_4$ nanoparticles, the IR-spectroscopic studies of samples 1-5 were conducted in the range of 400–4000 cm^{-1}. To analyze the experimental data (Fig. 10) we compared the characteristic bands of samples 4 and 5 with the bands of the initial substances (samples 1-3).

The molecules of linoleic acid and sunflower oil on the solid surface of Fe$_3$O$_4$ nanoparticles are under its influence. As a result, new absorption bands appear in the spectra (Fig. 10) and some characteristic absorption bands shift to the region of lower frequencies. This means the chemisorption of lipids, namely, linoleic acid and sunflower oil triglycerides on Fe$_3$O$_4$ NP surface. The absorption band of Fe–O bond with the maximum at ~532 cm^{-1} is observed in the spectrum of pure Fe$_3$O$_4$ (sample 1, Fig. 10a), which is in a good agreement with literature data (lit. ~530 cm^{-1}) [16, 17, 20, 28, 29]. The shift of this band maximum to ~584 cm^{-1} (samples 4 and 5, Figs. 10d and 10e) can be explained by the introduction of linoleic acid and sunflower oil surface molecules in the near-surface layer of Fe$_3$O$_4$ nanoparticles and their chemical interaction with iron cations (Figs. 2-8).
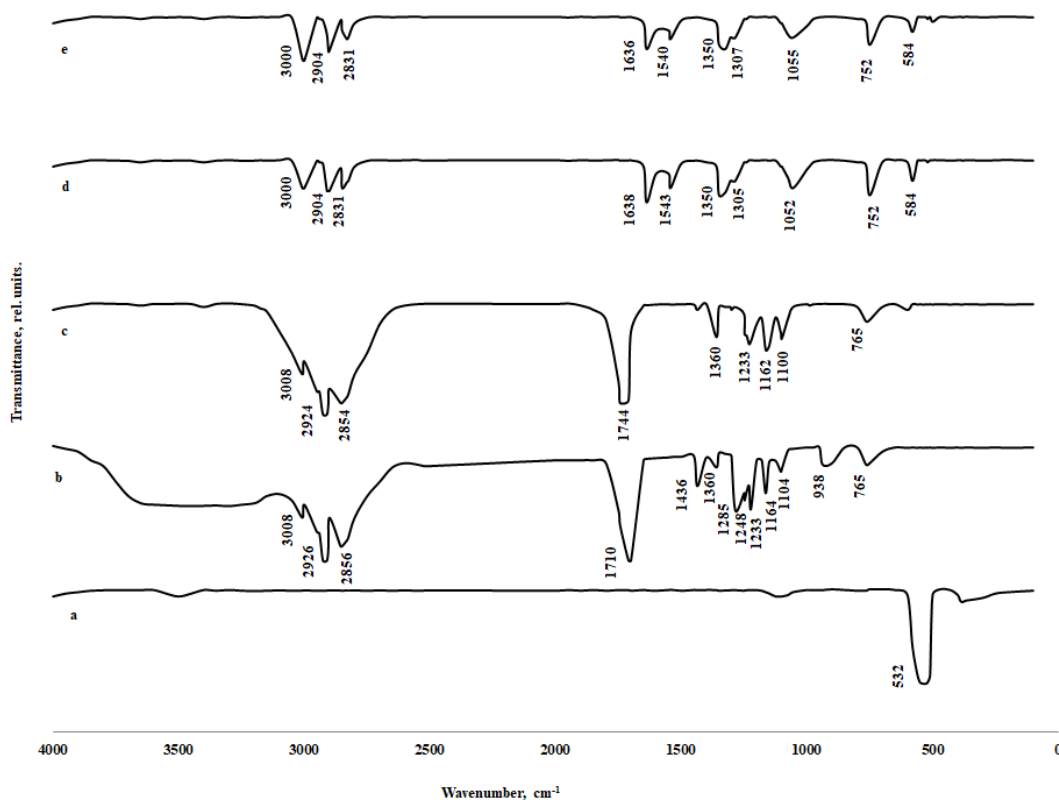
Fig. 10. FTIR spectra of the experimental samples: high-dispersive powder of Fe_3O_4 (a); linoleic acid (b); sunflower oil (c); Fe_3O_4 nanoparticles coated with linoleic acid (d)б and Fe_3O_4 nanoparticles coated with sunflower oil (e)

For lipid-Fe_3O_4 NP compositions the stretching vibration of C=O group have the greatest significance. The absorption band at 1710 cm^{-1} corresponds to an unexcited state of mentioned vibrations (Fig. 10b). For sunflower oil (Fig. 10c) we observe an intense peak of C=O vibrations in the area of 1744 cm^{-1} but this band disappears in the spectra of Fe_3O_4 nanoparticles coated with lipides (Fig. 10d, e). Moreover, the new bands appear at 1543 cm^{-1} (Fig. 10d), 1540 cm^{-1} (Fig. 10e), 1638 cm^{-1} (Fig. 10d), and 1636 cm^{-1} (Fig. 10e), which are typical of the stretching asymmetric (v_{as}) and symmetric (v_s) vibrations of the carboxylate group (COO$^-$). In other words, the lipids (carboxylic acids or triglycerides) are chemisorbed on the surface of Fe_3O_4 nanoparticles in carboxylate form (Figs. 7, 8, 10d, 10e) with the help of two oxygen atoms, which are symmetrically coordinated with the surface due to the electrostatic coordination interactions with Fe atoms. The result is the formation of chemically adsorbed lipid monomolecular layer (the first adsorption layer) on the NP surface (Figs. 2-8) [16, 17, 30, 31].

In the spectra of linoleic acid and sunflower oil, the intense bands with the maxima at 2926 and 2856 cm^{-1} (Fig. 10b); 2924 cm^{-1} and 2854 cm^{-1} (Fig. 10c) are observed. These peaks can be attributed to the asymmetric and symmetric vibrations of the C–H bond in CH$_2$ group.

Also, there is a band of deformation vibrations (δ) of –CH$_3$ group at ~1360 cm^{-1}; for linoleic acid this band is very weak [28-32].

The shift of absorption bands toward a lower field is observed in Figs. 10d and 10e (v_{as} = 2904 cm^{-1}; v_s = 2831 cm^{-1} and δ = 1350 cm^{-1}, respectively). The reasons are: (i) the hydrocarbon chains of linoleic acid and sunflower oil triglycerides in the monolayer (the first adsorption layer) surrounding the nanoparticles are under the influence of the near-surface layer of Fe_3O_4 NP and chemical interaction with Fe cations; (ii) the hydrophobic interaction of hydrophobic centers of the first adsorption layer with the hydrocarbon chains of linoleic acid and sunflower oil triglycerides occurred due to the dispersion forces contributes to the formation of the second adsorption layer on the surface of Fe_3O_4 nanoparticles [31, 32].

The unsaturated hydrocarbon chains in the structure of linoleic acid and sunflower oil triglycerides are represented by the stretching vibrations of–CH=CH– group at ~3008 cm^{-1} and deformation vibrations of C–H bond at ~765 cm^{-1} (Fig. 10b, c). For the structured Fe_3O_4 nanoparticles (Fig. 10d, e), there is a shift of these absorption bands toward v = 3000 cm^{-1} and δ = 752 cm^{-1}, respectively [28]. The reasons are: (i) the effect of Fe_3O_4 NP on the hydrocarbon chains of linoleic acid and

sunflower oil triglycerides in the formation of the first adsorption layer; (ii) the electrostatic interactions of the hydrophobic centers of the first adsorption layer with the alkyl matrix of triglycerides and the alkaline "tail" of the linoleic acid modeled on Van der Waals complexes. This contributes to the structuring of the "hydrophobic matrix" of the lipid-Fe_3O_4 NP complex and the formation of the second adsorption layer on the surface of Fe_3O_4 nanoparticles on which lipids (linoleic acid or sunflower oil) have already been adsorbed in the first adsorption layer [31, 32].

Three absorption bands corresponding to C▢O group are observed in each of linoleic acid and sunflower oil spectra: the intense band at 1164 and 1162 cm⁻¹ (Figs. 10b and 10c, respectively) and two less intensive bands at 1236 and 1233 cm⁻¹ (Figs. 10b and 10c, respectively); 1104 and 1100 cm⁻¹ (Figs. 10b and 10c, respectively). A doublet with the first peak at 1285 cm⁻¹ and the second one at 1248 cm⁻¹ is visible in the spectrum of linoleic acid (Fig. 10b). The first peak appears due to the combination of plane deformation ($\delta_{pd.}$) vibrations of O–H and C–O bonds. The second peak refers to the symmetric stretching vibrations of C–O bond. The asymmetric stretching vibrations typical of C–O bond of the linoleic acid carboxyl group appear on the doublet as the peak at 1436 cm⁻¹ [30-32].

The mentioned bands are absent in the spectra of Fe_3O_4 NP coated with lipids (Fig. 10d, e). At the same time, there are two new ones: at 1052 and 1305 cm⁻¹ (Fig. 10d); 1055 and 1307 cm⁻¹ (Fig. 10e), which are typical of plane deformation and stretching vibrations of C–O which interacts with polarized Fe_3O_4 nanoparticles (Figs. 4-6) [16, 17, 30-32].

The presence of the broad absorption band of average intensity in the spectrum of linoleic acid (Fig. 10b) in the range of 3200–3600 cm⁻¹ is associated with the characteristic vibrations of the surface OH⁻ groups. Out-of-plane deformation vibrations of O–H bond of the linoleic acid carboxyl group are observed at 938 cm⁻¹ but this band disappeared in the spectra of samples 3-5 (Fig. 10c, d, e). It is the confirmation of free hydroxyl groups absence on the surface of the lipid-Fe_3O_4 NP complex, as well as chemisorption of oleic acid and sunflower oil triglycerides on the surface of Fe_3O_4 nanoparticles (Figs. 2-8).

The results of IR spectroscopy and previous studies [16, 17, 30-32] confirm the formation mechanism of the first lipid adsorption layer on Fe_3O_4 nanparticles represented by four types: monodentate, bidentate (bridge), bidentate (chelate), and ionic interaction (Figs. 2-8) [16, 17, 20].

The difference in the wavenumber values (Δv_o) between the asymmetric and symmetric stretching vibrations of the carboxylate group (Fig. 10d, e) can be used to identify the type of interaction between COO⁻ group of lipid and Fe atom of Fe_3O_4 nanoparticles. The largest value Δv_o = (200–320) cm⁻¹ corresponds to the monodentate interaction, and the smallest one $\Delta v_o < 110$ cm⁻¹ – to bidentate (chelate). The value of 140–190 cm⁻¹ is characteristic of the bidentate (bridge) interaction. In this work, the Δv_o value of ~100 cm⁻¹ (1638 – 1543 = 95 cm⁻¹ for the sample d and 1636 – 1540 = = 96 cm⁻¹ for the sample (e)) indicates the bidentate structure, where two oxygen atoms of the lipid carboxyl group is coordinately bound with Fe atoms of Fe_3O_4 nanoparticles (Figs. 7, 8).

Thus, *the formation scheme of the first adsorption layer* on the nanoparticles surface is the chemisorption of lipid molecules on the Fe_3O_4 NP surface due to the electrostatic interactions of lipid polarized groups with the ionized particles and the coordination bonds of Fe atoms with oxygen of COO⁻ group. Moreover, the first adsorption layer is a combination of the symmetrically bound lipid molecules at an angle to the particles surface. Free hydrocarbon chains of sunflower oil and linoleic acid triglycerides bound with NP are perpendicular to the particles surface. These chains are superhydrophobic and they are a matrix for electrostatic hydrophobic interaction with hydrophobic "tails" of lipids.

The formation scheme of the second adsorption layer on the surface of Fe_3O_4 nanoparticles is the electrostatic interaction (due to dispersion forces) of the hydrophobic centers of the first adsorption layer with hydrophobic hydrocarbon "tails" of lipids (linoleic acid or sunflower oil triglycerides).

Thus, the mechanism of fat holding and fat binding capacity of Fe_3O_4 NP is the chemisorption of fats on the particles surface and can be represented by the two-layer coordination model.

3.2.2. X-ray diffraction analysis (XRD)

The crystal phases of Fe_3O_4 nanoparticles (sample 1) and nanoparticles coated with linoleic acid and sunflower oil (samples 4 and 5) were examined by X-ray diffraction analysis (Fig. 11).
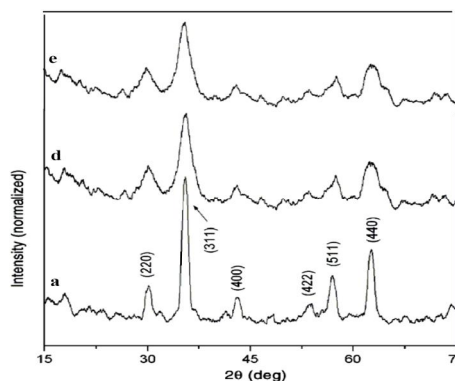

Fig. 11. X-ray diagrams of high-dispersive powder of Fe_3O_4 (a); Fe_3O_4 nanoparticles coated with linoleic acid (d) and Fe_3O_4 nanoparticles coated with sunflower oil (e)
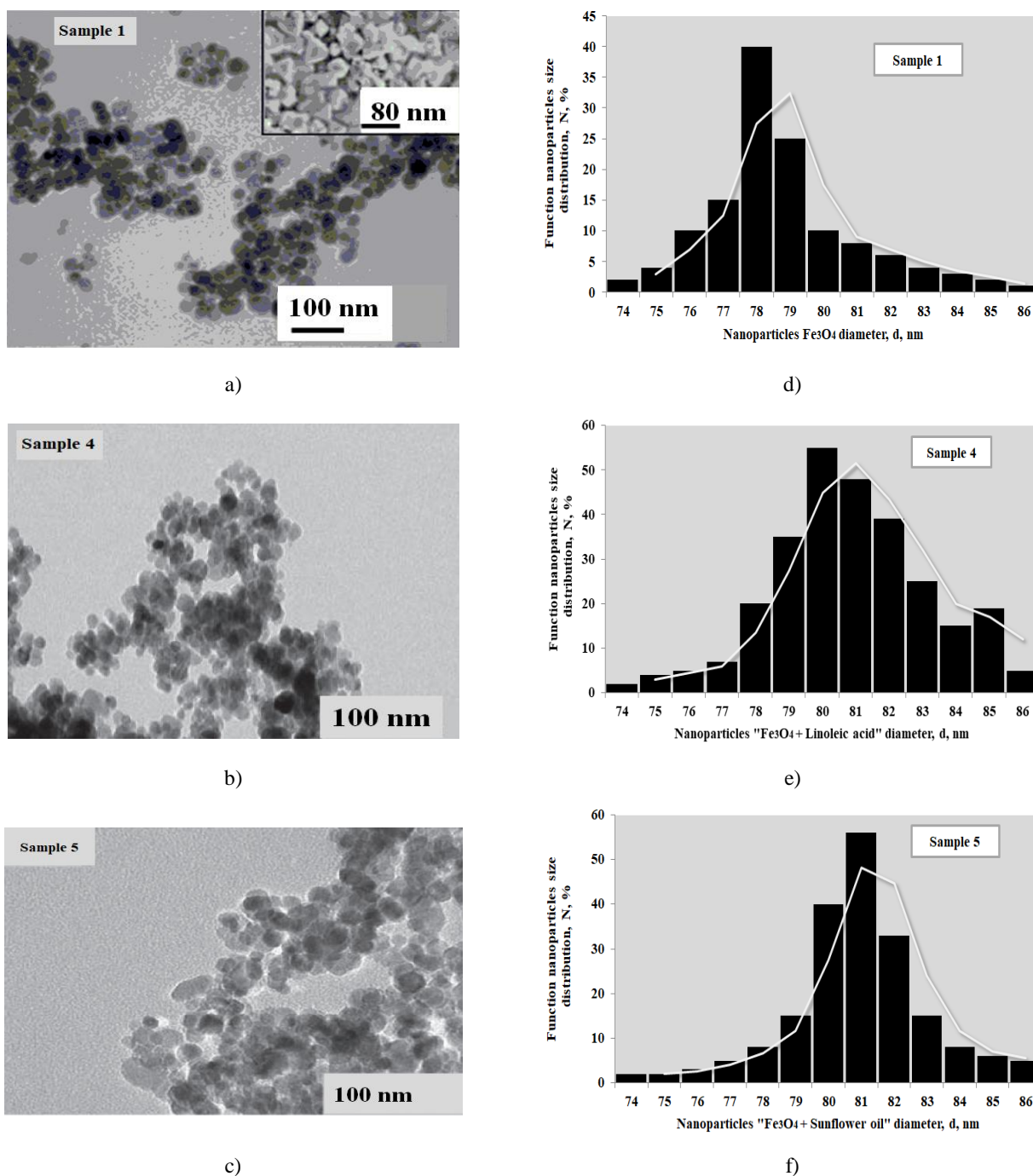
Fig. 12. TEM images (a, b, c) and nanoparticles size distribution (d, e, f)
of Fe_3O_4 high-dispersive powder (a, d); Fe_3O_4 nanoparticles coated with linoleic acid (b, e)
and Fe_3O_4 nanoparticles coated with sunflower oil (c, f)

The main bands of sample 1 (Fig. 11a) at $2\theta = 9.6°$; 30.42°; 35.59°; 43.42°; 54.58°; 57.60°, and 63.60° correspond to the diffraction of 220°; 311°; 400°; 422°; 511°, and 440°. They are typical of magnetite with a spinel structure and crystal lattice parameters of 0.83716(4) nm, while for an ordered and stoichiometric magnetite the suitable parameter is 0.83952(2) nm [26, 27, 33, 34]. The sharp peaks also suggest a good crystalline structure of Fe_3O_4 nanoparticles. Generally, sample 1 can be attributed to a highly dispersed spinel system.

There is also a widening of the bands in Fig. 11a, indicating a small size (nanosize) of particles and a slight tension of the crystalline structure. This affects the physico-chemical properties of Fe_3O_4 NP, in particular, by increasing their surface activity and reactivity, *e.g.*, the ability to interact with lipids of the food systems, namely, the higher fatty acids and triglycerides of fats. The established effect is associated with a small deficit of Fe^{3+} and Fe^{2+} cations both in tetrahedral and octahedral positions, which can be approximately evaluated as 5 %. But in general, this effect can be quite important and valuable for the modification of biopolymer matrices and stabilization of lipid-Fe_3O_4 systems.

Similar diffraction peaks are observed in the spectra of sample 4 (Fig. 11d) and sample 5 (Fig. 11e), *i.e.* the structure of cubic spinel remains unchanged for Fe_3O_4 coated with lipids. However, there is a widening of the diffraction peaks and a decrease in the signals intensity. These facts provide chemisorption of lipids on the NP surface and the effect of the surface molecules of linoleic acid and sunflower oil triglycerides due to their introduction in the near-surface layer of Fe_3O_4 nanoparticles and chemical interaction with Fe cations.

3.2.3. Morphological analysis of the experimental samples. Transmission electron microscopy (TEM)

The size of the particles and the morphology of the experimental samples 1, 4 and 5 (Fig. 12) were studied using a transmission electron microscopy (TEM).
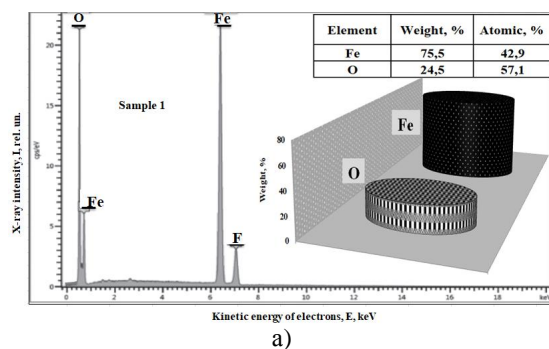
It is evident that all particles in experimental samples are nanosized, spherical in shape and have a uniform size distribution. Based on the obtained results, the particle distribution was calculated relative to the diameter. To determine the average values the particles number in the sample was at least 500. The established distribution function is rather narrow and symmetric, which validates the investigated systems as homogeneous ones with a low degree of polydispersity. The determined average sizes are: for sample 1 <d> ~78 ± 2.36 nm; for sample 4 <d> ~80 ± 2.57 nm; for sample 5 <d> ~81 ± 2.93 nm. The increase in the size of Fe_3O_4 particles of samples 4 and 5 compared with pure Fe_3O_4 (sample 1) is caused by adsorption of linoleic acid and sunflower oil on Fe_3O_4 NP surface and additionally confirms the proposed two-layer coordination model, the essence of which is the formation of two monomolecular layers on Fe_3O_4 NP surface. The total thickness (2*d*) is equal to two diameters of lipid molecules, *i.e.* for sample 4 2*d* = 2.2–2.5 nm; for sample 5 2*d* = 2.8–3.2 nm.

3.2.4. Elemental analysis of the experimental samples. Energy dispersive X-ray spectroscopy (EDX)

To confirm the chemisorption of lipids (linoleic acid and sunflower oil triglycerides) on particles surface the energy dispersive X-ray spectroscopy (EDX) was used. Using the EDX-spectra the elemental composition of the complex lipid-Fe_3O_4 NP was determined (Fig. 13).
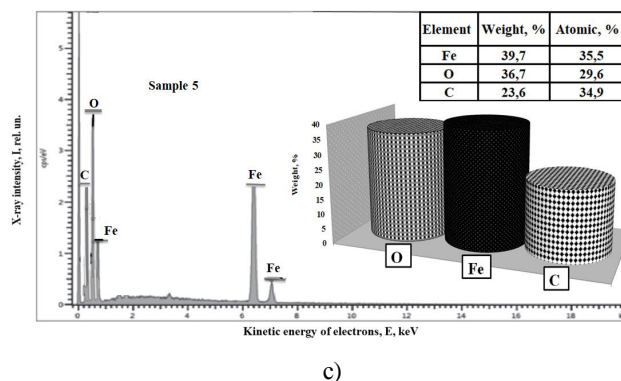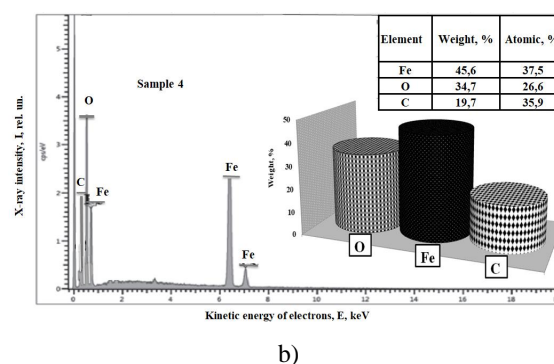
Element	Weight, %	Atomic, %
Fe	75,5	42,9
O	24,5	57,1

a)

Element	Weight, %	Atomic, %
Fe	45,6	37,5
O	34,7	26,6
C	19,7	35,9

b)

Element	Weight, %	Atomic, %
Fe	39,7	35,5
O	36,7	29,6
C	23,6	34,9

c)

Fig. 13. EDX spectra and the percentage of Fe, O, C of Fe_3O_4 high-dispersive powder (a); Fe_3O_4 nanoparticles coated with linoleic acid (b) and Fe_3O_4 nanoparticles coated with sunflower oil (c)
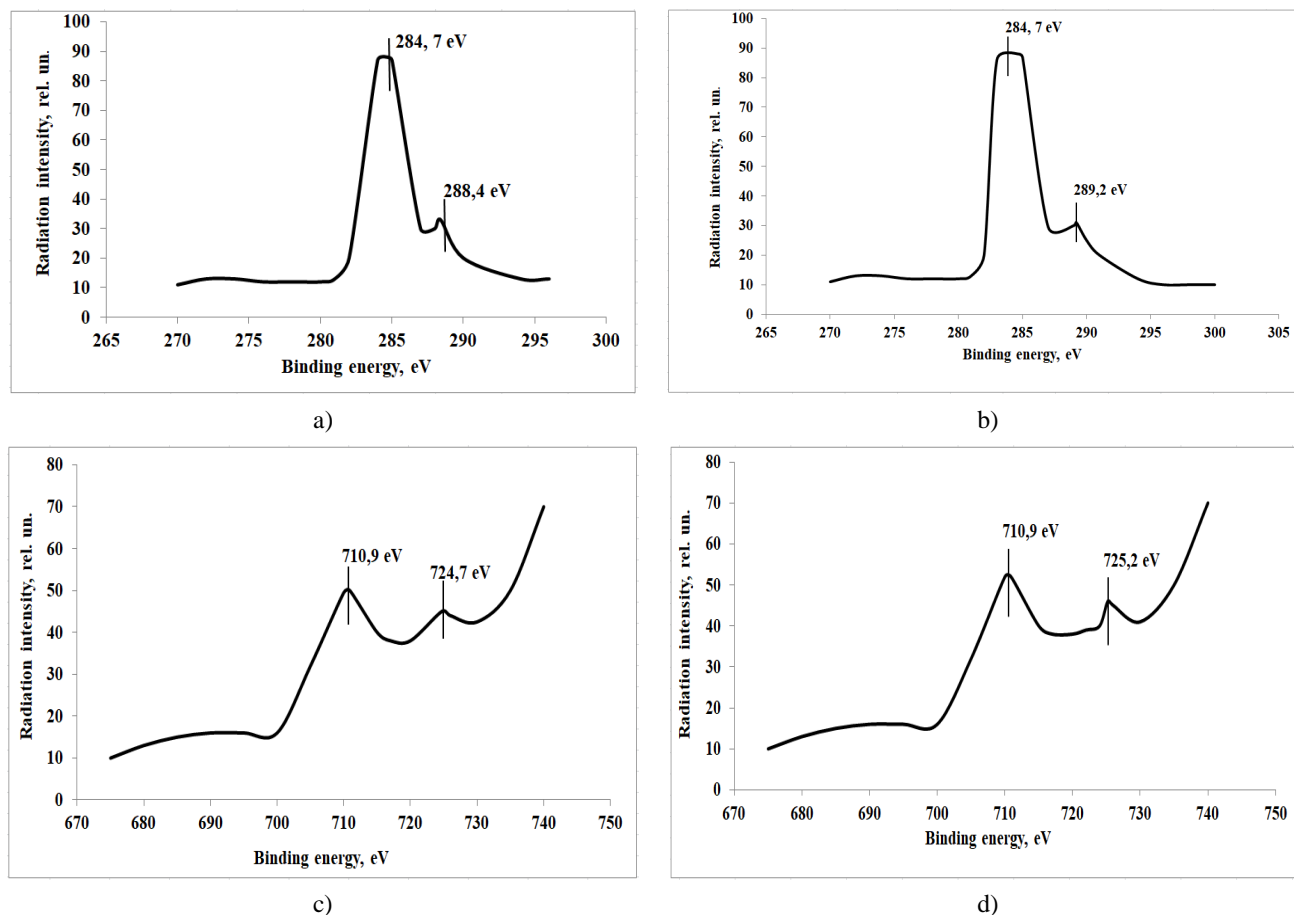
a)

b)

c)

d)

Fig. 14. XPS images of C 1s and Fe 2p internal electronic levels: C 1s level of Fe_3O_4 nanoparticles coated with linoleic acid (a); C 1s level of Fe_3O_4 nanoparticles coated with sunflower oil (b); Fe 2p level of Fe_3O_4 nanoparticles coated with linoleic acid (c) and Fe 2p level of Fe_3O_4 nanoparticles coated with sunflower oil (d)

In the spectra (Fig. 14a, b), there is no absorption band C 1s at 290 eV corresponding to carbon of carboxylic group (–COOH) [20]. This indicates the absence of free carboxylic acid or ester group of triglyceride on Fe_3O_4 nanoparticles coated with lipids. The peak at 284.7 eV (Fig. 14a, b) is attributed to the carbon atoms in the aliphatic chain (C–C); and the peaks at 288.4 eV (Fig. 14a) and 289.2 eV (Fig. 14b) are related to carboxylate (–COO–), which is in agreement with the received data from the literature [20, 35, 36].

The characteristic peak of oxides and iron hydroxides at 710.9 eV is not observed in the spectra (Fig. 14c, d). The peak characterizes the binding energy at basic level Fe $2p_{3/2}$ [20]. However, for samples 4 and 5 we observe the appearance of absorption band in the area of higher binding energies: 724.7 eV (Fig. 14c) and 725.2 eV (Fig. 14d). This absorption band is related to Fe carboxylate [20, 35, 36].

The obtained data give one more confirmation of the chemical structure of the experimental samples and indicate the formation of the chemical bonds between Fe atoms of Fe_3O_4 NP and oxygen atoms of lipids.

3.2.6. Thermogravimetric analysis (TGA)

The character of possible high-temperature transformations in samples 4 and 5 was investigated by using the thermogravimetric analysis [18, 20, 37, 38]. The results are represented in Fig. 15 in the form of thermogravimetric (TG) and the differential-thermo-gravimetric (DTG) curves.

Within the temperature range of 273–1173 K there are five temperature transformations:

– the first peak at 503 K (sample 4) and 500 K (sample 5) is accompanied by weight loss of 19.9 and 19.7 wt %, respectively. This peak is observed at the temperatures equal to the boiling points of linoleic acid ($T_b = 503$ K) and sunflower oil ($T_b = 500$ K). The weight loss is associated with the removal of free lipids (linoleic acid and sunflower oil) from the surface of Fe_3O_4 nanoparticles;
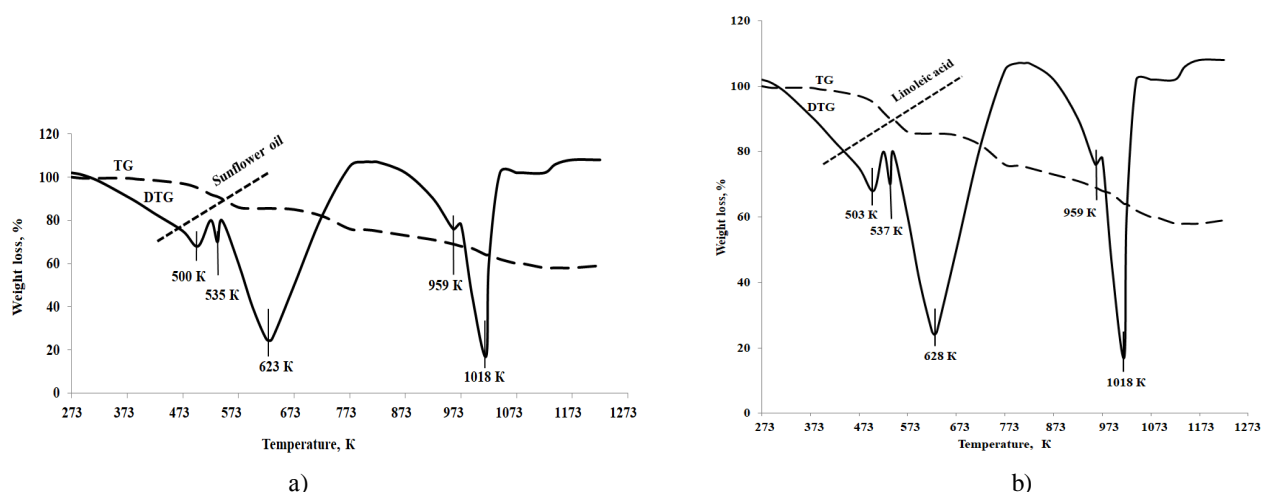
a)

b)

Fig. 15. Derivatograms of Fe_3O_4 nanoparticles coated with linoleic acid (a)
and Fe_3O_4 nanoparticles coated with sunflower oil (b)

– the second peak at 537 K (sample 4) and 535 K (sample 5) with weight loss of 12.2 and 12.0 wt %, respectively, may be associated with the desorption of the second adsorption layer formed due to the electrostatic interactions of the hydrophobic centers of the first adsorption layer and the hydrocarbon "tails" of the higher fatty acids (in particular, linoleic) and triglycerides of free fat (in particular, sunflower oil). This fact coincides with the models of two-layer modification of nanoparticles by the various chemical reagents [19, 20, 40-42];

– the third peak at 628 K (sample 4) and 623 K (sample 5) is accompanied by weight loss of 22.3 and 21.6 wt %, respectively. The mass loss is connected with the desorption of the first adsorption layer, which is formed due to the stronger (compared with the hydrophobic interaction in the second layer) electrostatic interactions of lipid polarized groups with ionized Fe_3O_4 NP and the coordination bonds of Fe atoms of Fe_3O_4 nanoparticles with oxygen of COO^- group of "hydrophilic heads" of fat (in particular, sunflower oil triglycerides) and the higher fatty acids (in particular, linoleic acid). This is in agreement with literature data [19, 20, 40-42] and additionally confirms the proposed two-layer coordination model;

– the fourth peak at 959 K (samples 4, 5) is accompanied by the insignificant weight loss of 2.6 wt % related to the phase conversion of double Fe(II) and Fe(III) oxide (Fe_3O_4) into metastable Fe(III) oxide γ-Fe_2O_3 with the cubic structure. Further heating provides the transformation of γ–modification into diamagnetic rhombohedral structure (hematite). This is in good agreement with literature data [41, 42];

– the fifth peak at 1015 K (samples 4, 5) is associated with weight loss of 14 wt %, due to the possible deoxidation of FeO of Fe_3O_4 NP.

Thus, the TGA method, along with other investigation methods regarding the mechanism of lipids chemisorption on the surface of Fe_3O_4 nanoparticles, confirms the proposed two-layer coordination model.

4. Conclusions

The interaction mechanism of Fe_3O_4 nanoparticles with linoleic acid and 1-linoleyl-2-oleoyl-3-linolenoyl-glycerol has been grounded. The mechanism is presented by the two-layer coordination model. The first adsorption layer is formed on the nanoparticle surface due to the electrostatic interactions of polarized lipid groups with ionized Fe_3O_4 particles and the coordination bonds of Fe atoms of Fe_3O_4 nanoparticles with the carbonyl and hydroxyl oxygen atoms of the carboxyl groups of free fatty acids, as well as with oxygen atoms of ester groups of triglycerides. The second adsorption layer occurs due to the electrostatic hydrophobic interactions of the hydrophobic centers of the first monolayer and the aliphatic side chains of the acyl residues of triglycerides and the alkyl components of the free fatty acids.

Different methods of analysis (FTIR, XRD, TEM, EDX, XPS, TGA) regarding the mechanism of lipids chemisorption on the surface of Fe_3O_4 nanoparticles, confirmed the proposed two-layer coordination model.

The obtained results will allow to simulate the processes of fat holding and fat binding capacity in various technological and food systems, as well as to improve the functional and technological characteristics of fat-containing compositions and the quality of finished products.

Further investigations concerning chemisorption of the higher fatty acids, fats, and oils of various origin and chemical composition on the surface of Fe_3O_4 nanoparticles are of great interest.

References

[1] Rogov I., Tokaev Eh., Kovalev Yu.: Ispolzovanie Syria s Vysokim Soderzhaniem Pishchevykh Volokon v Tekhnologii Dieticheskikh Miasnykh Produktov. Agroniitehimmp, Moskva 1988.

[2] Citrusovye volokna Herbacel AQ Plus – tip N: Specifikacii dlya pishchevyh dobavok i receptury, 2013. http://specin.ru/kletchatka/109.htm

[3] Pavlovich-Abril A., Rouzaud-Sández O., Romer-Baranzini A. L. *et al.*: J. Food Quality, 2015, **38**, 30. https://doi.org/10.1111/jfq.12103

[4] Varastegani B., Zzaman W., Yang T.: J. Food Quality, 2015, **38**, 175. https://doi.org/10.1111/jfq.12129

[5] Http://www.pischevie-volokna.ru

[6] Rodríguez R., Jiménez A., Fernández-Bolaños J. *et al.*: Trends Food Sci. Tech., 2006, **17**, 3. https://doi.org/10.1016/j.tifs.2005.10.002

[7] Chang T., Wang S., Wang C., Shi L. *et al.*: J. Food Quality, 2014, **37**, 339. https://doi.org/10.1111/jfq.12096

[8] https://www.ingredientsnetwork.com/Herbacel_AQ_Plus_Citrus_manu_vegan_Cleanlabel_emulsions-file072775.pdf

[9] Beriain M., Gómez I., Ibáñez F. *et al.*: Improvement of the Functional and Healthy Properties of Meat Products [in:] Holban A.-M., Grumezescu A.-M. (Eds.), Food Quality: Balancing Health and Disease. Academic Press, NY 2018, 1-74. https://doi.org/10.1016/B978-0-12-811442-1.00001-8

[10] Domoroshchenkova M., Demyanenko L., Kamysheva T.: Maslozhyrovaya Prom., 2007, **4**, 24.

[11] Lai W., Khong N., Lim S. *et al.*: Trends Food Sci. Tech.., 2017, **59**, 148. https://doi.org/10.1016/j.tifs.2016.11.014

[12] Heymans R., Tavernier I., Dewettinck K., Van der Meeren P.: Trends Food Sci. Tech., 2017, **69A**, 13. https://doi.org/10.1016/j.tifs.2017.08.015

[13] Paglarini C., Furtado G., Biachi J. *et al.*: J. Food Eng., 2018, **222**, 29. https://doi.org/10.1016/j.jfoodeng.2017.10.026

[14] Ramachandraiah K., M.-J. Choi, G.-P. Hong: Trends Food Sci. Tech., 2018, **71**, 25. https://doi.org/10.1016/j.tifs.2017.10.017

[15] Ilyuha N., Barsova V., Kovalenko V., Tsyhanovska I.: Vost. Evr. Zh. PeredovyhTekhnol., 2010, **6**, 32.

[16] Tsykhanovska I., Alexandrov A., Evlash V. *et al.*: East. Eur. J. Adv. Technol., 2018, **2**, 70. https://doi.org/10.15587/1729-4061.2018.126358

[17] Tsykhanovska I., Alexandrov A., Evlash V. *et al.*: East. Eur. J. Adv. Technol., 2018, **4**, 61. https://doi.org/10.15587/1729-4061.2018.140048

[18] Drmota A., Kosak A., Znidarsik A.: Mater. Technol., 2008, **42**, 79.

[19] Mahdavi M., Ahmad M., Haron M. *et al.*: Molecules, 2013, **18**, 7533. https://doi.org/10.3390/molecules18077533

[20] Zhang L., He R., Gu H.-C.: Appl. Surf. Sci., 2006, **253**, 2611. https://doi.org/10.1016/j.apsusc.2006.05.023

[21] Chernyshova I., Ponnurangam S., Somasundaran P.: Langmuir, 2011, **27**, 10007. https://doi.org/10.1021/la2017374

[22] Alexandrov A., Tsykhanovska I., Evlash V. *et al.*: East. Eur. J. Adv. Technol., 2017, **5**, 61. https://doi.org/10.15587/1729-4061.2017.111522

[23] Tsykhanovska I., Skurikhina L., Evlash V. *et al.*: Ukr. Food J., 2018, **7**, 379. https://doi.org/10.24263/2304-974X-2018-7-3-4

[24] Tsykhanovska I., Alexandrov A., Evlash V. *et al.*: Eureka: Life Sci., 2018, **4**, 63. https://doi.org/10.21303/2504-5695.2017.00511

[25] Tsykhanovska I., Alexandrov A., Evlash V. *et al.*: Eureka: Life Sci., 2018, **2**, 67. https://doi.org/10.21303/2504-5695.2018.00611

[26] Russ J.: Fundamentals of Energy Dispersive X-Ray Analysis. Butterworth-Heinemann 1984.

[27] ICCD: The International Centre For Diffraction Data. http://www.icdd.com/

[28] Wang L.: Advances in nanocomposites, 2008, 34, 289.

[29] Hajdu A., Illes E., Tombacz E., Borbath I.: Colloid. Surf., 2009, **347**, 104. https://doi.org/10.1016/j.colsurfa.2008.12.039

[30] Shen Y., Tang J., Nie Z. *et al.*: Sep. Purif. Technol., 2009, **68**, 312. https://doi.org/10.1016/j.seppur.2009.05.020

[31] Skopenko V., Civadze A., Savranskij L., Garnovskij A.: Koordinacionnaya Khimia. Akademkniga, Moskva 2007.

[32] Steed J., Atwood J.: Supramolecular Chemistry. John Wiley & Sons, Ltd., Chichester 2009.

[33] Andrade F. R. D. *et al.*: Geol. USP, Sér. cient., 2016, **16**, 19. https://doi.org/10.11606/issn.2316-9095.v16i2p19-24

[34] Kazeminezhad I., Mosivand S.: Acta Phys. Polonica A., 2014, **125**, 1210. https://doi.org/10.12693/APhysPolA.125.1210

[35] Yamashita T., Hayes P.: Appl. Surf. Sci., 2008, **254**, 2441. https://doi.org/10.1016/j.apsusc.2007.09.063

[36] Poulin S., França R., Moreau-Bélanger L.: J. Phys. Chem. C, 2010, **114**, 10711. https://doi.org/10.1021/jp100964x

[37] Levitin E., Vedernikova I., Onoprienko T., Tsykhanovska I.: Farmakom, 2007, **1**, 61.

[38] Sahoo Y., Pizem H., Fried T. *et al.*: Langmuir, 2001, **17**, 7907. https://doi.org/10.1021/la010703+

[39] Shen L., Laibinis P., Hatton T., Langmuir, 1999, **15**, 447. https://doi.org/10.1021/la9807661

[40] Yee C., Kataby G., Ulman A. *et al.*: Langmuir, 1999, **15**, 7111. https://doi.org/10.1021/la990663y

[41] Bozort R: Ferromagnetism. Izd-vo standartov, Moskva 1986.

[42] Goss C.: Phys. Chem. Minerals, 1988, **16**, 164. https://doi.org/10.1007/BF00203200

ДОСЛІДЖЕННЯ МЕХАНІЗМУ ВЗАЄМОДІЇ ЛІНОЛЕВОЇ КИСЛОТИ ТА 1-ЛІНОЛЕЇЛ-2-ОЛЕОЇЛ-3-ЛІНОЛЕНОЇЛГЛІЦЕРИНУ З НАНОЧАСТИНКАМИ Fe_3O_4

Анотація. *Обґрунтовано механізм взаємодії наночастинок Fe_3O_4 з лінолевої кислотою та з 1-лінолеїл-2-олеоїл-3-ліноленоїлгліцерином, який представлений моделлю «двошарової координації». Методами ІЧ-Фур'є спектроскопії, трансмісійної електронної мікроскопії, енергодисперсійної рентгенівської спектроскопії, рентгенівської фотоелектронної спектроскопії, рентгенофазового і термогравіметричного аналізу вивчений механізм взаємодії лінолевої кислоти і соняшникової олії з наночастинками Fe_3O_4.*

Ключові слова: *наночастинки Fe_3O_4, лінолева кислота, 1-лінолеїл-2-олеоїл-3-ліноленоїлгліцерин, соняшникова олія, хемосорбція.*